Physico-chemical and antibacterial studies on silver doped nano-hydroxyapatite

C.S. CIOBANU[a], E. ANDRONESCU[b,c], A.M. PRODAN[b,d,e], L. PALL[b,f], A. COSTESCU[g,h,i], P. LE COUSTUMER[h,], F. HUNEAU[i, j], L. MARUTESCU[k], N.I. ENE[k], R. TRUSCA[l], E. S. BARNA[g], S. L. ICONARU[a,g*]

[a]*National Institute of Materials Physics, 105 bis Atomistilor, P.O. Box MG 07, 077125, Bucuresti-Magurele, Romania,*
[b]*University Politechnica of Bucharest, Faculty of Applied Chemistry and Materials Science,1-7 Polizu Street, P.O. Box 12-134, 011061 Bucharest, Romania*
[c]*AOSR, Splaiul Independentei nr. 54, sector 5, 050094 Bucuresti, Romania*
[d]*Carol Davila University of Medicine and Pharmacy, 8 Eroii Sanitari, sector 5, Bucharest, Romania*
[e]*Emergency Hospital Floreasca, 8 Calea Floresca, sector 1, Bucharest, Romania*
[f]*ICMCB-CNRS, UPR9048, 87 Avenue du Docteur Schweitzer 33608, Pessac Cedex France*
[g]*University of Bucharest, Faculty of Physics, 405 Atomistilor, CP MG – 1, 077125, Bucuresti-Magurele, Romania*
[h]*Universite Bordeaux, EA 4592 Géoressources & Environnement, EGID, 1 allée F. Daguin 18, 33607 Pessac Cedex France*
Universite de Corse Pascal Paoli, Faculté des Sciences et Techniques, Laboratoire d'Hydrogéologie, F 20250 Corte, France
j CNRS UMR 6134 SPE, , F 20250 Corte, France[k]*Faculty of Biology, Microbiology Department, University of Bucharest, Ale. Portocalelor 1-3, 60101, Bucharest, Romania*
[l]*SC Metav-CD SA, 31 C.A. Rosetti , Bucharest, Romania*

In this paper we show that preparation of Ag doped hydroxyapatite by an adapted co-precipitation method at 100°C has several advantages over other techniques. Specifically, it can generate highly crystalline nanopowder Ag:HAp which could be used for implantable medical devices. The XRD of HAp (x_{Ag} = 0) and Ag:HAp (x_{Ag} = 0.05, and x_{Ag} = 0.4) also demonstrates that powders obtained by co-precipitation at 100^0C exhibit the apatite characteristics with good crystal structure and no new phase or impurity is found. The SEM results suggested that Ag^+ doping had little influence on the morphology and dimension of the samples. It can be seen that all the samples consist of elipsoidal particles. The antibactericidal activity of Ag:HAp-NPs with x_{Ag} = 0, x_{Ag} = 0.05, and x_{Ag} = 0.4 on *Bacilus* and *E.coli ESBL 1576* were presented. The Ag:HAp-NPs with x_{Ag} = 0.05, and x_{Ag} = 0.4 inhibited the biofilm development both by the *gram-positive* (*Staphylococcus aureus* 0364) and the *gram-negative* (*Providencia stuartii 1116*) strains. On the other hand, our studies have shown that Ag:HAp with x_{Ag} = 0 had no antibacterial activity against *gram-positive* and *gram-negative* bacteria.

(Received July 9, 2013; accepted July11, 2013)

Keywords: Silver, Hydroxyapatite, Antibacterial activity

1. Introduction

Today, nanoparticles are used in many fields such as photonic, electronic, catalytic, chemical, and biosensor areas because of their size effects compared to those of bulk metal and molecular compounds [1-15]. In the living environment there are many microorganisms, which in certain circumstances can infect humans. Due to improper use of antibiotic therapy, in the last two decades we have seen an increase in bacterial resistance to antibiotics, and as a result new pharmaceuticals methods are being investigated for increasing the inhibitory and bactericidal effect of antibiotics [16- 19].

Silver nanoparticles have been used for centuries for their inhibitory and bacteriostatic properties. It has been demonstrated that Ag^+ binds to functional groups of proteins, leading to protein denaturation [20-23]. Bactericidal effect of silver nanoparticles is not fully understood. It is assumed that one of the mechanisms involved in the inhibitory and bacteriostatic effect refers to electrostatic attraction between negatively charged bacterial cells and positively charged silver nanoparticles [18-21].

Some studies on the effect of these nanoparticles on antibiotics, reported production of nanosized silver particles with different morphologies and sizes, using different methods. Silver nanoparticles were prepared using chemical reduction from aqueous solutions of silver nitrate. The aqueous solutions used contained a mixture of hydrazine hydrate and sodium citrate as reductants and sodium dodecyl sulfate as stabilizer [24].

In this study we used silver nanoparticles to investigate the inhibitory and bactericidal effects against bacterial strains such as *Staphylococcus aureus* 0364 (*gram-positive*) and *Providencia stuartii 1116 (gram-negative).* The results of these experiments demonstrated

that silver-doped hydroxyapatite nanoparticles increase the inhibitory and bactericidal effect on the studied microorganisms.On the other hand, the structure and morphological properties of the obtained samples were systematically characterized by X-ray diffraction (XRD) and scanning electron microscopy (SEM). The XRD of $Ca_{10-x}Ag_x(PO_4)_6(OH)_2$ demonstrate that powders made by co-precipitation at 100^0C exhibit the apatite characteristics with good crystal structure and no new phase or impurity is found.

2. Materials and methods

2.1. Synthesis of Ag^+ doped hydroxyapatite

All the reagents for synthesis, including ammonium hydrogen phosphate [$(NH_4)_2HPO_4$], calcium nitrate [$Ca(NO_3)_2{\cdot}4H_2O$], and silver nitrate $AgNO_3$ were purchased from Alpha Aesar and used without further purification.

The $Ca_{10-x}Ag_x(PO_4)_6(OH)_2$, with $x_{Ag} = 0$, $x_{Ag} = 0.05$, and $x_{Ag} = 0.4$, ceramic powder was prepared (Ca/P molar ratio: 1.67) using $Ca(NO_3)_2{\cdot}4H_2O$ and $(NH_4)_2HPO_4$ by co-precipitation. A mixture of 0.5 M ammonium hydrogen phosphate and 1.67 M calcium nitrate tetrahydrate solutions was stirred constantly for 2 h by a mechanical stirrer at 100 °C. The pH was constantly adjusted and kept at 10 during the reaction. After 2 h the precipitate was washed several times with deionised water. The resulting material was dried at 100 ^{0}C for 72 h in an electrical air oven.

For silver doped hydroxyapatite nanoparticles the ratio [Ca+Ag] /P was 1.67. $AgNO_3$ and $Ca(NO_3)_2{\cdot}4H_2O$ were dissolved in deionised water to a final volume of 300 ml [Ca+Ag] – containing solution. $(NH_4)_2HPO_4$ was dissolved in deionised water to a final volume of 300 ml P- containing solution. The [Ca+Ag] – containing solution was stirred at 100 °C for 30 minutes. The P- containing solution with a pH of 10 (adjusted by NH_3) was added drop by drop into the [Ca+Ag] – containing solution and stirred for 2 h. The pH value was constantly adjusted at 10 during the reaction. Afterwards the precipitate was washed several times with deionised water. The resulting material was dried at 100 ^{0}C for 72h.

2.2. Sample characterization

The X-ray diffraction measurements for $Ca_{10-x}Ag_x(PO_4)_6(OH)_2$ samples were recorded using a Bruker D8 Advance diffractometer, with nickel filtered Cu K_α (λ=1.5418 Å) radiation, and a high efficiency one-dimensional detector (Lynx Eye type) operated in integration mode. The diffraction patterns were collected in the 2θ range between 15^o – 140^o, with a step of 0.02^o and 34 s measuring time per step. Scanning electron microscopy (SEM) study was performed on a HITACHI S2600N-type microscope equipped with an energy dispersive X-ray attachment (EDAX/2001 device).

2.3. The in vitro antibacterial and antifungal activity

The antimicrobial activities of the tested substances were determined against ATCC reference and clinical microbial strains, *i.e. gram-positive* (*Bacillus subtilis,*) and *gram-negative* (E. coli 1576bacterial strains. The microbial strains identification was confirmed by aid of VITEK II automatic system. VITEK cards for identification and susceptibility testing were inoculated and incubated according to the manufacturer's recommendations. The results were interpreted using the software version AMS R09.1.

The tested substances were solubilised in DMSO and the starting stock solution was of 1000 µg/mL concentration. The qualitative screening was performed by an adapted disk diffusion method [25-29].

The assessment of the complexes influence on the microbial ability to colonize an inert substratum was performed by the micro-titer method. For this purpose, the microbial strains have been grown in the presence of two-fold serial dilutions of the tested compounds performed in liquid nutrient broth/YPG, distributed in 96-well plates and incubated for 24 hours at 37 °C for bacterial strains, respectively for 48 hours at 28 °C for fungal strains. At the end of the incubation period, the plastic wells were emptied, washed three times with phosphate buffered saline (PBS), fixed with cold methanol and stained with 1% violet crystal solution for 30 minutes. The biofilm formed on plastic wells was resuspended in 30% acetic acid. The intensity of the coloured suspensions was assessed by measuring the absorbance at 490 nm. [30-33].

3. Results and discussions

3.1. Structure, formation and morphology of pure HAp and Ag:HAp

The designed unit formula of the doped HAp is: $Ca_{10-x}Ag_x(PO_4)_6(OH)_2$, with $0 \le x \le 0.4$. The XRD patterns, presented in Figure 1, show the characteristic peaks of hydroxyapatite for each sample, according to ICDD-PDF no. 9-432, represented at the bottom of the figure, as reference. No other crystalline phases were detected beside this phase (Figure 1).

Figure 1 shows the XRD (patterns) of pure HAp-NPs, Ag:HAp-NPs ($x_{Ag} = 0.05$, and $x_{Ag} = 0.4$) and the standard data for the hexagonal hydroxyapatite, respectively. For pure HAp-NPs ($x_{Ag} = 0$), the diffraction peaks can be well indexed to the hexagonal $Ca_{10}(PO_4)_6(OH)_2$ in $P6_3m$ space group (ICDD-PDF No. 9-432). In the case of Ag:HAp-NPs samples ($x_{Ag} = 0.05$, and $x_{Ag} = 0.4$), the characteristic diffractions of hexagonal HAp are still obvious, and no other phases related with doped component can be detected. The XRD of HAp and Ag:HAp nanoparticles also demonstrate that powders made by co-precipitation at 100^0C exhibit the apatite characteristics with good crystal structure and no new phase or impurity is found.

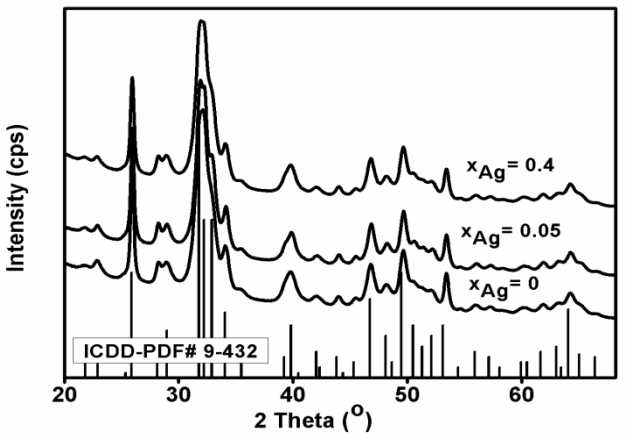

Fig. 1. Comparative representation of the experimental XRD patterns of the Ag:HAp samples synthesized x_{Ag} = 0, x_{Ag} = 0.05, and x_{Ag} = 0.4, and the characteristic lines of hydroxyapatite according to the ICDD - PDF number 9-432

SEM images provide direct information about the size and typical shape of the as-prepared samples. The morphology of the $Ca_{10-x}Ag_x(PO_4)_6(OH)_2$ nanoparticles, with $0 \leq x \leq 0.4$ was investigated by SEM. In Fig. 2 SEM images of $Ca_{10-x}Ag_x(PO_4)_6(OH)_2$, with x_{Ag} = 0, x_{Ag} = 0.05 and x_{Ag} = 0.4 are shown.

The results suggested that the doping by Ag^+ has little influence on the sample's morphology and dimensions. It can be seen that all the samples consist of ellipsoidal particles. These particles are non-aggregated with narrow distribution with particles from 5 nm to 80 nm.

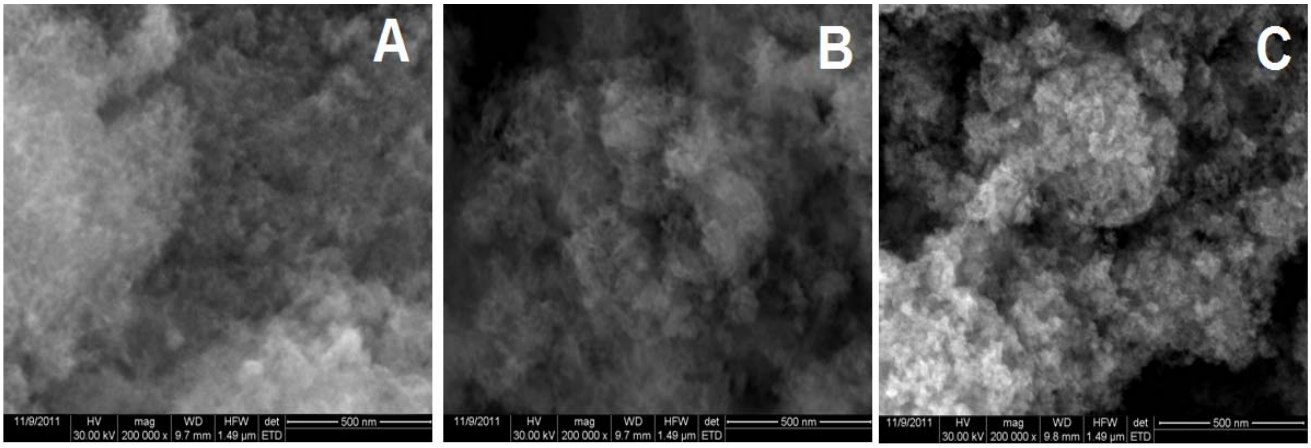

Fig. 2. SEM images of the Ag:HAp samples with x_{Ag} = 0 (A), x_{Ag} = 0.05(B) and x_{Ag} = 0.4(C).

3.2. Antibacterial tests

The microbial species of clinical interest, often involved in biofilm associated diseases belong to a very large spectrum, from the *gram- positive* (*Bacilus*) to the *gram-negative* pathogens (*E.coli ESBL 1576*) [**34**]. The antibacterial activity of Ag:HAp-NPs was tested against the *gram-negative* bacteria *E coli ESBL 1576* and the *gram-positive* bacteria *Bacilus.*The inhibitory activity of the $Ca_{10-x}Ag_x(PO_4)_6(OH)_2$ samples, with x_{Ag} = 0, x_{Ag} = 0.05 and x_{Ag} = 0.4 are presented in Figs. 3-4.

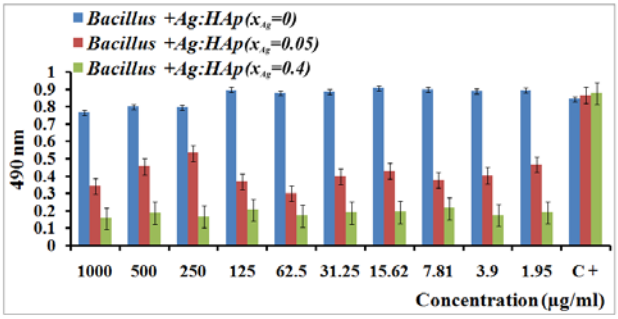

Fig. 3. The quantitative assay of the inhibitory effect of Ag:HAp-NPs on biofilms developed on the inert substratum by Bacilus, quantified by the A_{490nm} values.

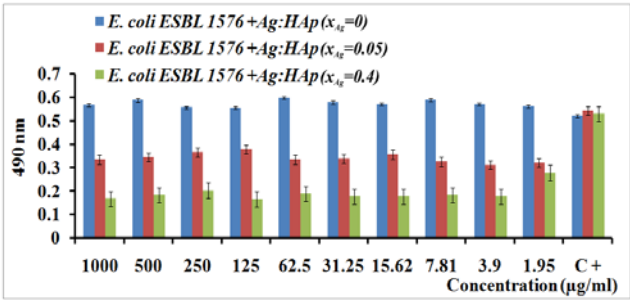

Fig. 4. The quantitative assay of the inhibitory effect of Ag:HAp-NPs on biofilms developed on the inert substratum by E.coli ESBL 1576, quantified by the A_{490nm} values.

Ag:HAp-NPs with x_{Ag} = 0.05 and x_{Ag} = 0.4 showed a significant inhibitory effect against both bacterial strains, for all tested concentrations. The antibacterial effect of Ag:HAp-NPs on the *gram-negative* bacteria *E.coli ESBL 1576* was slightly less noticeable than that on the *gram-positive* bacteria *Bacilus* for all concentrations. The *E.coli ESBL 1576* and *Bacilus* strains were not inhibited in the presence of Ag:HAp-NPs with x_{Ag} = 0. Our results showed that the samples with x_{Ag} = 0.4 possess the highest antibacterial activity for all tested concentration.

3. Conclusions

The XRD analysis of Ag:HAp-NPs synthesized at room temperature using an adapted co-precipitation method demonstrated that the obtained powders exhibit the apatite characteristics with good crystal structure and no new phase or impurity is found.

A very good antibacterial activity against *Bacilus* and *E Coli ESBL 1576* was observed in the presence of Ag:HAp-NPs with x_{Ag} = 0.05 and x_{Ag} = 0.4. For the Ag:HAp-NPs with x_{Ag} = 0, samples the inhibitory activity is not present. The antimicrobial assays revealed that Ag:HAp-NPs (x_{Ag} = 0.05 and x_{Ag} = 0.4) have a great potential to be used as antimicrobial agents against microorganisms.

Acknowledgements: The authors would like to thank Professor Mariana Carmen Chifiriuc of Microbiology Immunology Department, Faculty of Biology, and University of Bucharest for assistance with antimicrobial tests and for the constructive discussions. This work was supported by the Ministery of Educations of the Romania, project No: C2-06 under program CEA-IFA and „Program Nucleu PN 45".

References

[1] C.D. Jones, M.J. Serpe, L. Schroeder, L.A. Lyon, J. Am. Chem. Soc. **125**, 5292 (2003).
[2] L.M. Liz-Marzán, Langmuir **22,** 32 (2006).
[3] P. Liljeroth, D. Vanmaekelbergh, V. Ruiz, K. Kontturi, H. Jiang, E. Kauppinen, B.M. Quinn, J. Am. Chem. Soc. **126,** 7126 (2004).
[4] P.V. Kamat, J. Phys. Chem. B **106,** 7729 (2002).
[5] A. Costescu, I. Pasuk, F. Ungureanu, A. Dinischiotu, M. Costache, F. Huneau, S. Galaup, P. Le Coustumer, D. Predoi, Dig. J. Nanomater. Bios. **5**(4), 989 (2010).
[6] D. Predoi, R.V.Ghita, F. Ungureanu, C.C. Negrila, R. A. Vatasescu-Balcan, M. Costache, J. Optoelectron. Adv. Mater. **9**(12), 3827 (2007).
[7] C. S. Ciobanu, S. L. Iconaru, F. Massuyeau, L. V. Constantin, A. Costescu, D. Predoi, Journal of Nanomaterials, 2012, doi:10.1155/2012/942801.
[8] F. Frumosu, S.L. Iconaru, D. Predoi, Dig. J. Nanomater. Bios. **6**(4), 1859 (2011).
[9] C.S. Ciobanu, E. Andronescu, D. Predoi, J. Optoelectron Adv. Mater. **13**(7), 821 (2011).
[10] C. S. Ciobanu, E. Andronescu, A. Stoicu, O. Florea, P. Le Coustumer, S. Galaup, A. Djouadi, J.Y. Mevellec, I. Musa, F. Massuyeau, A. M. Prodan, Khalid Lafdi, R. Trusca, I. Pasuk, D. Predoi, Dig. J. Nanomater. Bios. **6**(2), 609 (2011).
[11] D. Predoi, S. Derible, H. Duflo, J. Optoelectron Adv. Mater. **11**(6), 852 (2009).
[12] D. Predoi, M. Barsan, E. Andronescu, R. A. Vatasescu-Balcan, M. Costache, J. Optoelectron Adv. Mater. **9**(11), 3609 (2007).
[13] D. Predoi, Dig. J. Nanomater. Bios. **2**(1), 169 (2007).
[14] D. Predoi, C.M.Valsangiacom, J. Optoelectron Adv. Mater. **9**(6), 1797 (2007).
[15] D. Predoi, Dig. J. Nanomater. Bios. **5**(2), 373 (2010).
[16] T. N. Kim, Q. L. Feng, J. O. Kim, J. Wu, H. Wang, G.. C.Chen, et al. J. Mater. Sci. Mater. Med. **9**, 129 (1998).
[17] K. H. Cho, J. E. Park, T. Osaka, S. G. Park, Electrochim. Acta. **51**,956 (2005).
[18] C. S. Ciobanu, F. Massuyeau, L. V. Constantin, D. Predoi, Nanoscale Res. Lett. **6**, 613 (2011).
[19] C. S. Ciobanu, S.L. Iconaru, P. Le Coustumer, L. V. Constantin, D. Predoi, Nanoscale Res. Lett. Accepted Manuscript (2012)
[20] J. R. Morones, J. L. Elechiguerra, A. Camacho, K. Holt, J. B. Kouri, J. T. Ramirez, et al. Nanotechnology **16**, 2346 (2005).
[21] S. Shrivastava, T. Bera, A. Roy, G. Singh, P. Ramachandrarao, D. Dash, Nanotechnology **18**, 9 (2007).
[22] S.K. Gogoi, P. Gopinath, A. Paul, A. Ramesh, S.S. Ghosh, A. Chattopadhyay, Langmuir **22**, 9322 (2006).
[23] Q.L. Feng, J. Wu, G.Q. Chen, F.Z. Cui, T.N. Kim, J.O. Kim, J. Biomed. Mater. Res. **52**, 662 (2000).
[24] S. Mandal, S. Karumugam, R. Pasricha, M. Sastry. Bull. Mate. Sci. **28**, 503 (2005).
[25] C. Limban, M.C.Chifiriuc, Int. J. Mol. Sci. **12**(10), 6432 (2011).
[26] C. Limban, L. Marutescu, M. C. Chifiriuc, Molecules. **16**(9), 7593 (2011).

[27] C. Saviuc, A. M. Grumezescu, A. Holban, C.Bleotu, C. Chifiriuc, P. Balaure, V. Lazar, Biointerface Res. App. Chem. **1**(3), 111 (2011).
[28] M.C. Chifiriuc, R. Palade, A. M. Israil, Biointerface Res. App. Chem. **1**(6), 209 (2011).
[29] L. Marutescu, C. Limban, M. C. Chifiriuc, A.-V. Missir, I.C. Chirita, M. T. Caproiu, Biointerface Res. App. Chem. **1**(6), 236 (2011).
[30] A. M. Grumezescu, D. E. Mihaiescu, D. E. Mogoşanu, M. C. Chifiriuc, V. Lazăr, I. Călugărescu, V. Trăistaru, Optoelectron. Adv. Mater.-Rapid. Commun. **4**(11), 1798 (2010).
[31] C. Chifiriuc, V. Lazăr, C. Bleotu I. Călugărescu, A. M. Grumezescu, D. E. Mihaiescu, D. E. Mogoşanu, Dig. J. Nanomater. Bios. **6**(1), 37 (2011).
[32] C. Saviuc, A. M.Grumezescu, E.Oprea, V. Radulescu, L. Dascalu, M. C.Chifiriuc, M.Bucur, O. Banu, V. Lazar, Biointerface Res. App. Chem. **1**(1), 015 (2011).
[33] C. Saviuc, A. M. Grumezescu, M.C. Chifiriuc, C. Bleotu, G.Stanciu, R. Hristu, D. Mihaiescu, V. Lazăr, Biointerface Res. App. Chem. 1(1), 031 (2011).
[34] V. Lazar, C. Chifiriuc, Rom Arch of Microb & Immunol. **69**,125 (2010)

*Corresponding author: simonaiconaru@gmail.com